

## Article

# Photoacoustic Spectroscopy Combined with a Multipass Circular Cell to Detect Low Concentrations of Ammonia

Oscar E. Bonilla-Manrique <sup>1,\*</sup>, Alejandro Pérez Gonzalez-Banfi <sup>1</sup>, Jorge Viñuela Pérez <sup>2</sup> and Gabriele Dessena <sup>3</sup>

<sup>1</sup> Electronic Technology Department, Universidad Carlos III de Madrid, 28911 Leganés, Spain; 100451011@alumnos.uc3m.es

<sup>2</sup> School of Computing and Digital Media, London Metropolitan University, 166-220 Holloway Road, London N7 8DB, UK; jorge.vinuelap@gmail.com

<sup>3</sup> Department of Aerospace Engineering, Universidad Carlos III de Madrid, 28911 Leganés, Spain; gdessena@ing.uc3m.es

\* Correspondence: obonilla@ing.uc3m.es

**Abstract:** Photoacoustic spectroscopy (PAS) has become a valuable technique for trace gas detection due to its high sensitivity and potential for miniaturization. This study presents the development and evaluation of a near-infrared PAS system using a 1532 nm semiconductor laser and a multipass cell (MPC) designed to enhance the optical path and thereby improve the detection of ammonia (NH<sub>3</sub>). The minimum detection limit was determined to be 770 ppb, with a normalized noise equivalent absorption (NNEA) coefficient of  $1.07 \times 10^{-8} \text{ W cm}^{-1} \text{ Hz}^{-1/2}$ . While competitive with similar PAS systems, these results indicate that mid-infrared technologies still offer superior detection thresholds. The findings suggest that while this near-infrared setup may not yet match the sensitivity of systems using quantum cascade lasers or QEPAS, it offers notable advantages in terms of simplicity, cost, and potential for field deployment. The system's configuration makes it a viable and efficient tool for industrial gas monitoring and real-time environmental applications, with future improvements likely to come from transitioning to the mid-infrared region and advancing laser stabilization and miniaturization techniques.

**Keywords:** photoacoustic; multipass circular cell; low concentration detection; ammonia; optical spectroscopy; near infrared



Academic Editor: Monica Gallo

Received: 14 May 2025

Revised: 5 June 2025

Accepted: 13 June 2025

Published: 16 June 2025

**Citation:** Bonilla-Manrique, O.E.; Pérez Gonzalez-Banfi, A.; Viñuela Pérez, J.; Dessena, G. Photoacoustic Spectroscopy Combined with a Multipass Circular Cell to Detect Low Concentrations of Ammonia. *Appl. Sci.* **2025**, *15*, 6727. <https://doi.org/10.3390/app15126727>

**Copyright:** © 2025 by the authors. Licensee MDPI, Basel, Switzerland. This article is an open access article distributed under the terms and conditions of the Creative Commons Attribution (CC BY) license (<https://creativecommons.org/licenses/by/4.0/>).

## 1. Introduction

Gas detection is an indispensable component in a wide range of industries, including environmental monitoring, medical diagnostics, human health, and process optimization [1]. In industrial scenarios [2], accurate identification and quantification of gas concentrations are critical to maintaining safe operating conditions. In the healthcare sector, gas detection techniques have found applications in non-invasive diagnostics. For instance, the analysis of volatile organic compounds (VOCs) in exhaled breath can be utilized to detect and monitor a range of diseases [3–5]. In the domain of environmental monitoring, gas detection plays a crucial role in the continuous monitoring of air quality and the quantification of greenhouse gas (GHG) emissions [6]. This capacity is imperative for evaluating pollutant levels, enforcing environmental regulations, and informing policy decisions aimed at mitigating the impact of anthropogenic activities on climate change. Consequently, measures are being implemented to reduce greenhouse gas emissions, particularly carbon dioxide (CO<sub>2</sub>) [7]. Among these, the introduction of carbon-neutral fuels such as hydrogen or ammonia (NH<sub>3</sub>) has garnered significant attention [8,9]. Ammonia (NH<sub>3</sub>) is a promising

option for cleaner energy sources because it has the potential to be a fuel that does not produce CO<sub>2</sub> [8]. Nonetheless, it can also be very dangerous to people and the environment if it is not handled correctly. High concentrations can cause irritation to the eyes, skin and lungs. It can even cause death. It can also pollute the air and water [10].

Consequently, the generation of “green ammonia” becomes a possibility. Green ammonia is produced using renewable energy sources such as wind or solar power, through the electrolysis of water [11,12]. This hydrogen is then combined with nitrogen from the air to produce NH<sub>3</sub>. The accurate and efficient detection of NH<sub>3</sub> is crucial, and infrared absorption spectroscopy is a useful tool for this purpose [13]. In particular, tunable diode laser absorption spectroscopy (TDLAS) allows for the accurate and rapid detection of gases, due to its ability to tune the laser to specific wavelengths. This makes it a valuable tool in industrial and environmental applications [14,15]. However, its effectiveness can be affected by optical or environmental interference, and it requires constant calibration and maintenance. Alternatively, indirect detection techniques, such as photoacoustic spectroscopy (PAS), have emerged as a viable alternative [16,17]. A key strength of photoacoustic spectroscopy lies in its high sensitivity and accuracy in detecting extremely low concentrations, as it directly measures the thermal energy released by light absorption through the generation of acoustic waves [18]. This capability ensures its applicability in complex environments where other techniques might fail due to optical interferences. Furthermore, photoacoustic spectroscopy demonstrates high sensitivity in high-pressure, high-temperature environments and under normal environmental conditions [19–21]. The classical PAS configuration utilizes resonant cells to enhance detection, particularly cylindrical cells. Quartz-enhanced photoacoustic spectroscopy (QEPAS) is a highly sensitive detection method for trace gases, even in difficult environmental conditions, reaching levels in the order of parts per billion [22–24]. It uses a quartz resonator to detect acoustic signals generated by light absorption. Another technique that enhances the averaging element is cantilever-enhanced photoacoustic spectroscopy (CEPAS), which uses a thin cantilever as a sensor that responds mechanically to light absorption [25,26]. Furthermore, optical microphones based on interferometry enable the precise measurement of changes in the cantilever [19]. Finally, multipass cells represent another variation of PAS, offering significant advantages in terms of sensitivity, selectivity, and flexibility compared to resonant cells [27,28].

In this study, we propose a sensor for NH<sub>3</sub> detection in the near-infrared using a distributed-feedback continuous-wave (DFB-CW) telecommunication laser in an innovative PAS system based on a commercial multipass circular cell (MPC) of reduced size, suitable for PAS system implementation. The characterization and optimization of the MPC-PAS system will be presented, and its efficacy will be validated by detecting different trace concentrations of ammonia in nitrogen in terms of sensitivity.

## 2. Materials and Methods

### 2.1. Photoacoustic Effect and Multipass Cell

The photoacoustic effect was discovered by Alexander Graham Bell, who detected an acoustic signal by modulating a light source and causing it to impinge on a sample contained in a closed cell. It consists of the absorption of modulated light by the sample, leading to an increase in its internal energy. This energy is transferred to adjacent molecules, which are heated and undergo a process of expansion and contraction. This generates pressure variations, producing acoustic waves [16], which can be detected by sensors such as microphones. This process is illustrated in Figure 1.

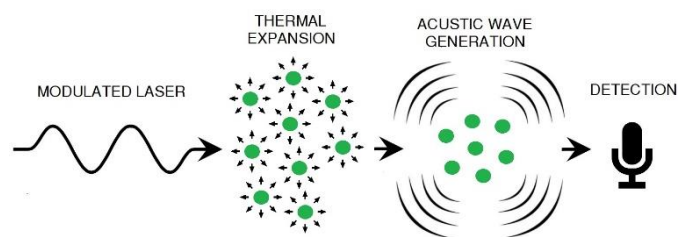


**Figure 1.** Generation of the photoacoustic effect.

The photoacoustic effect can be explained in three fundamental processes: first, the absorption of light radiation, which depends on the properties of the material, such as the absorption coefficient and the length of the optical path; second, transformation of electromagnetic energy into heat, which depends on the quantum efficiency of the sample; and finally, the diffusion of heat up to the threshold at which acoustic waves are produced is the result of the interplay between diffusivity, conductivity, and specific heat capacity. While several authors have described in detail the photoacoustic effect inside a cavity, the photo-induced signal can be expressed generally as follows:

$$S \propto \frac{P * \alpha}{f * V} \quad (1)$$

where  $P$  is the optical power of the light source,  $f$  is the modulation frequency,  $\alpha$  is the absorption coefficient of the gas molecules, and  $V$  is the interaction volume. As described in Equation (1), there are different ways to improve the photoacoustic signal. One of the options is to increase the optical path by using multipass cells. The MPC-PAS technique has been shown to offer a significant advantage in terms of enhancing the sensitivity and accuracy of gas detection [29–32]. By having the light beam pass multiple times through the sample, the total amount of energy absorbed by the gas molecules is increased, leading to the generation of a more intense acoustic signal. This capability enables the detection of extremely low gas concentrations, thereby improving the signal-to-noise ratio of the system. MPC, a key component of the system, enhances efficiency without necessitating an increase in laser power, rendering it well-suited for applications that demand high precision and trace detection, such as environmental monitoring and industrial process detection. The multipass cell's enhanced optical lengthens the effective optical path, making it particularly advantageous for dilute or low-concentration samples, where the photothermal signal may be weak. Additionally, this cell's extended optical path enhances selectivity by increasing interaction time and suppressing undesired background signals. The MPC-PAS is implemented by a multipass cell (Figure 2), which is characterized by its small size (10 cm diameter) and its composition of 45 parabolic mirrors inside the cell [29,33].

These mirrors facilitate multiple reflections, thereby increasing the optical path of the system and enhancing its advantages. The cell's stability, attributable to its resistance to thermal expansion, surpasses that of alternative photoacoustic cell types, rendering it particularly well suited for environments where temperature control is challenging [30]. This cell's attributes include its small size, adaptable path length, straightforward alignment, and versatility in sensing techniques. The reduction in size and volume of the cell offers significant advantages for the development of rapid and portable gas detection systems. Conventional cells typically exhibit stringent requirements regarding distance, axial flip angle, and mirror tilt to meet operational conditions. In contrast, the optical cell depicted in Figure 2 allows for straightforward modification of the optical path length by adjusting the orientation angle of the input laser beam, rendering it well suited for the analysis of gaseous species with distinct absorption lines. Although this type of cell is traditionally used for

direct absorption spectroscopy, the present study proposes to use it as a circular resonator within a photoacoustic configuration. The cell is equipped with a series of gold-coated spherical mirrors in a circular configuration, integrated within a single toroidal component, thereby significantly streamlining the optical alignment procedure and ensuring superior beam shaping. The copper ring is manufactured by diamond machining (Kugler Ltd., Salem, Germany), yielding a high-quality aspheric surface suitable for optical applications due to its low roughness of a few nanometers. The surface reflectivity is enhanced by the deposition of a 200 nm thick gold layer on the surface [29].

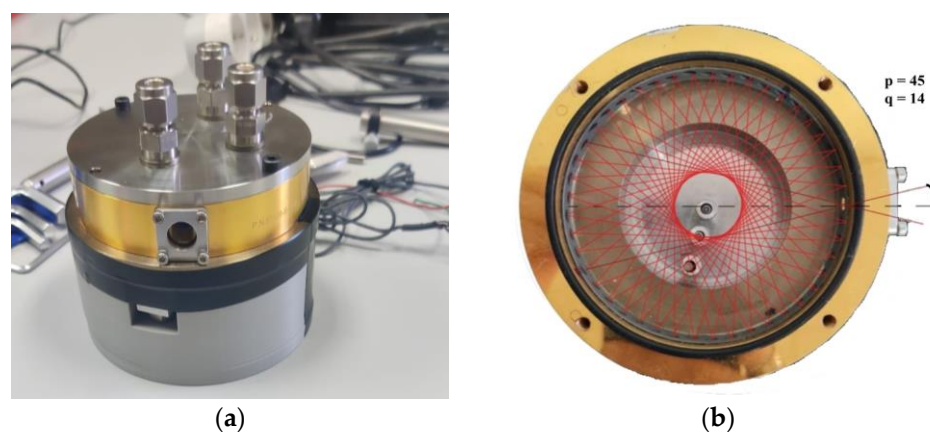


**Figure 2.** Multipass cell. (a) Cell on custom-designed mounting for easy installation. (b) Diagram of the reflection polygon due to multiple reflections inside the cell.

## 2.2. Wavelength Selection and Gas Mixing

In order to successfully implement the MPC-PAS system, it is essential to carefully select the laser emission wavelength to match the absorption characteristics of ammonia in nitrogen. It is fundamental to be aware of the spectral characteristics of the gas to be detected, as well as potential interference from other gases. In this instance, the emphasis is on the near-infrared spectral region corresponding to 1532 nm. For this purpose, the HITRAN (high-resolution transmission molecular absorption database) spectroscopic database has been used. At this wavelength, no significant interference from other common gases such as  $\text{H}_2\text{O}$ ,  $\text{CO}_2$ ,  $\text{CH}_4$ , or  $\text{CO}$  is detected, even at high concentrations. This has been corroborated by experimental validation, which identified the main absorption lines in the 1532 nm range, as illustrated in Figure 3.

This spectrum was simulated using the HITRAN database and measured by laser scanning. The different concentrations were generated from two gas cylinders: one containing pure  $\text{N}_2$  as the carrier gas and the other containing  $\text{NH}_3$  at a certified concentration of 5000 ppm in  $\text{N}_2$ . Both gas flows were regulated by two mass flow controllers (F-201CV-AGD-22-K, Bronkhorst, Ruurlo, Netherlands), which were also used to perform dilutions, while the total flow was kept constant [34]. It should be noted that  $\text{NH}_3$  is a common gas that easily adheres to surfaces and pipes due to its physical and chemical properties. It has been observed that  $\text{NH}_3$  can also exhibit capillary condensation in pipes or porous materials, where gas molecules condense in small pores or capillaries at pressures below the bulk saturation pressure. This effect is especially pronounced in tight spaces or when the temperature is low. For this reason, a system based on materials that prevent this effect, such as Teflon (polytetrafluoroethylene or PTFE) and gold coating, were used. Ammonia, a polar gas, exhibits minimal interaction with the non-polar surface of Teflon, thereby ensuring minimal adsorption and accumulation of ammonia on surfaces, a crucial consideration in this application. Constant gas replenishment prevented cumulative heating within the

cell, while the gas mixture was fluxed through the gas cell by means of a valve system, a pressure controller, and a rotary pump.

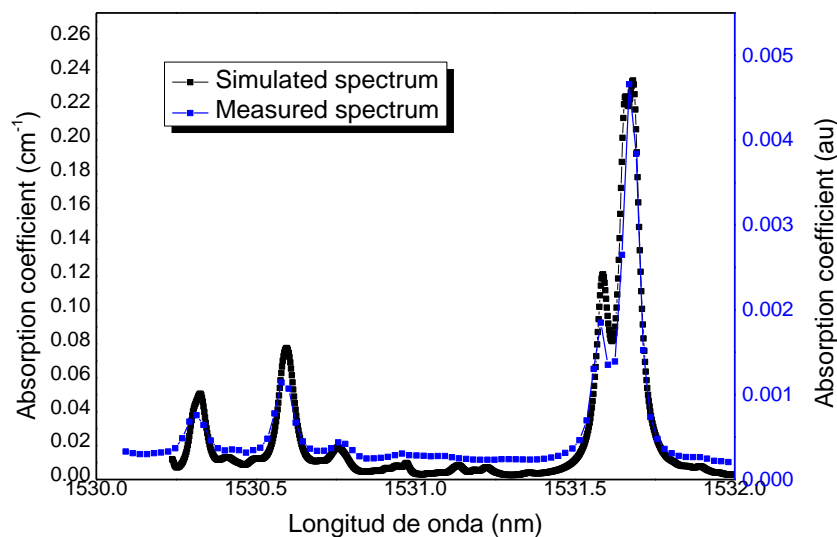


**Figure 3.** Ammonia absorption lines in the 1530 nm range. Simulated spectrum from the HITRAN database and measured by laser scanning [19].

### 2.3. Experimental Setup

The MPC-PAS architecture implemented for the experimental validation presented in this paper is shown in Figure 4.

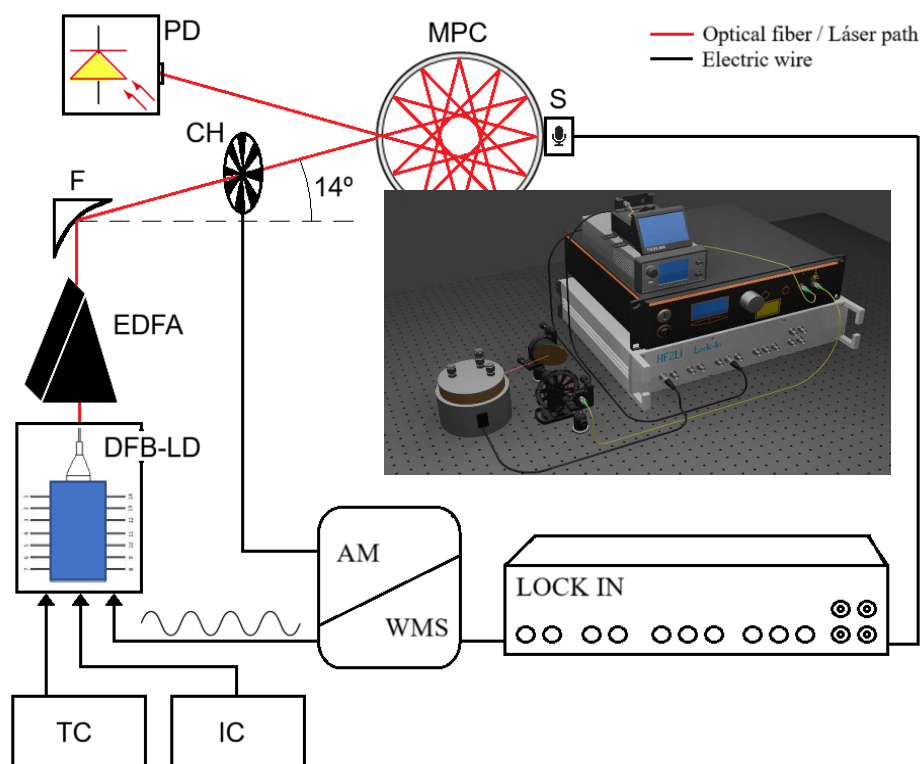


**Figure 4.** Experimental architecture MPC-PAS implemented. DFB-LD, DFB laser diode at 1532 nm; TC, temperature controller; IC, current controller; EDFA, optical amplifier; PD, reference photodetector; CH, chopper modulator; F, parabolic mirror; MPC, multipass circular cell; S, acoustic sensor; Loc-In, lock-in amplifier; AM/WMS, control, data acquisition, and processing system. 3D diagram of the implemented system.

The complete system is based on the classical PAS, which implements a semiconductor laser emitting in the NIR at a wavelength equal to the absorption footprint of the gas under study. A near-infrared distributed feedback laser (DFBLD-1530-20, Eblana, Dublin, Ireland) is used. The laser diode emits at 1532 nm with an output power of 20 mW, supporting a maximum operating current of 105 mA and an operating temperature range of 15 to 40 °C. It has a wavelength–temperature tuning coefficient of 0.1 nm/°C and a fine current coefficient of 10 pm/mA. In addition, it has a thermoelectric cooler for precise thermal stability and a thermistor for accurate temperature monitoring. A compact laser diode current and temperature driver (CLD1015, Thorlabs, Newton, NJ, USA) is used to precisely adjust these parameters. The operating temperature was set to 26 °C, and a current of 94.8 mA was applied to tune the emission to the NH<sub>3</sub> absorption line. Under these conditions, the measured optical output power was 10 mW. The optical signal was amplified using an erbium-doped fiber amplifier (EDFA) (CEFA-C-PB-HP, Keopsys, Lannion, France) at a 700 mA operating current, which provides an optical power gain of approximately 7 dB, to obtain an optical power of 50 mW.

The laser beam was focused on the gas cell by a 100 mm focal length, gold-coated parabolic mirror (MPD269-M01, Thorlabs, Newton, NJ, USA). As previously described, a circular multipass cell was chosen, specifically, the IRcell-4m model from IRsweep (Stäfa, Switzerland). The IRcell-4m is an instrument designed for infrared absorption spectroscopy and offers a 4 m optical path in a compact design. It uses highly reflective mirrors on its inner walls that allow multiple reflections of the light beam, thus extending the optical path without increasing the physical size of the cell. The bottom cover of the cell underwent modification, resulting in the drilling of three holes at equal distances from the center of the cell. These perforations enabled the installation of three sensors to detect the photoacoustic signal generated within the cell. This modification also permitted the adjustment of the sensors' height within the confines of the cell. Three identical capacitive microphones (FG-23329-P18, -53 dB, BW = 10 kHz Knowles Electronics, Itasca, IL, USA) were installed equidistantly (1 cm) from the center of the cell as shown in Figure 5. The MPC was installed on a custom-made support manufactured using a 3D printer, which facilitates straightforward installation and alignment. The top cover was outfitted with three gas inlets/outlets to regulate the concentration and flow within the cell.

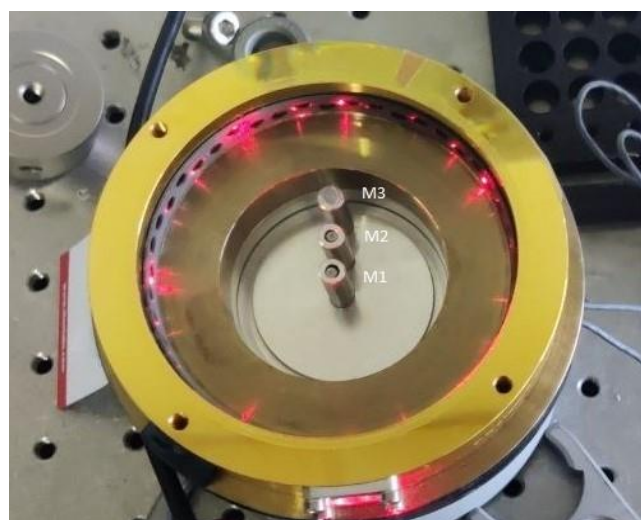


**Figure 5.** Installation of the three electrical microphones inside the multipass cell, parallel to the optical beam.

Two modes of operation were used. In the first, focused on cell characterization, the optical beam was modulated by a mechanical chopper (MC2000B with MC1F10HP,

BW = 10 kHz, Thorlabs, Newton, NJ, USA). This was controlled by a TTL reference signal at different frequencies provided by a lock-in amplifier (Lock-in HF2LI, Zurich Instruments, Zurich, Switzerland). A low-frequency voltage ramp (1 Hz) was applied to the current driver to scan the laser wavelength around the absorption line. The other mode was used for sensor characterization. A sinusoidal modulation was superimposed on the low-frequency voltage ramp via the driver's external input, producing rapid optical frequency modulation. The slow voltage signal was generated by directly changing the current parameters of the driver using software developed in LabView 2020, while the sinusoidal signal was obtained at one of the output ports of the lock-in amplifier generator. For both sensing detection modes, the signal was sent to the lock-in amplifier and demodulated at the 1st and 2nd harmonic, respectively. The integration time was set to 10 ms with an 8th order low pass filter. The lock-in amplifier was interfaced directly with a computer, and the signal was recorded and processed using custom software developed in LabView.

### 3. Results

#### 3.1. Characterization of the Circular Multipass Cell

To implement the MPC-PAS system, the first step was to analyze the cell to define its resonant modes in order to maximize the photoacoustic signal generated inside the cell. These are standing waves that can be formed inside the cell due to multiple reflections of the incident light. These resonant modes are determined by the dimensions and optical properties of the cell, as well as the boundary conditions imposed by the surrounding materials. The resonant modes can have different shapes and spatial distributions depending on the cell geometry and material properties. It is important to note that the proper selection of resonant modes is crucial to optimize the performance of a resonant cell in photothermal spectroscopy. As previously stated, three capacitive microphones were installed inside the cell, spaced 1 cm apart and symmetrically positioned around the center as shown in Figure 5. The laser beam was incident inside the cell and it was modulated by a chopper (MC2000B, BW = 10 kHz, Thorlabs, Newton, NJ, USA). The modulation frequency was varied in a range from 1.5 kHz to 9 kHz with a step of 20 Hz. The results obtained for the microphones are shown in Figure 6, where three main resonance modes can be observed at approximate frequencies: 4000 Hz, 6800 Hz, and 8000 Hz.

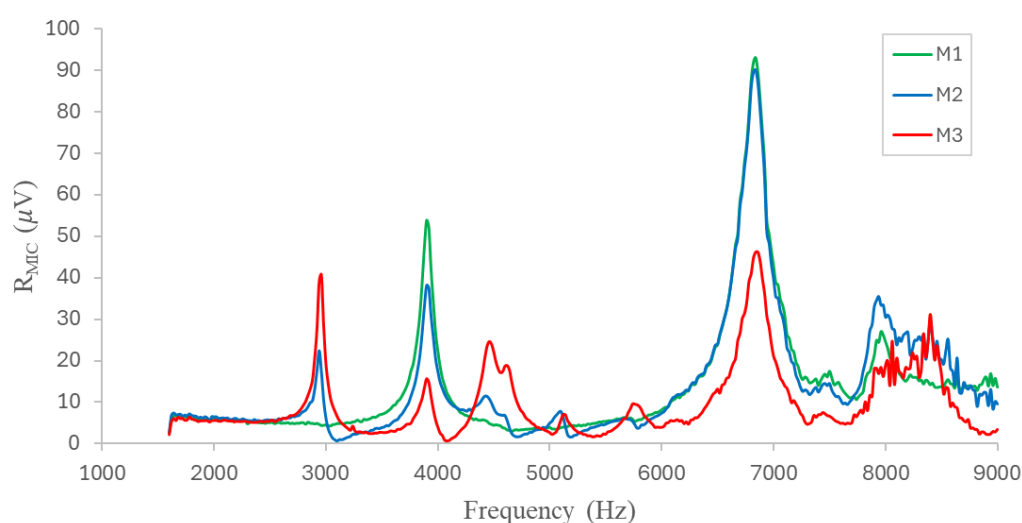


**Figure 6.** Resonant modes inside the cell identified by the three microphones.

Due to its instability and very poor response, the resonant mode near 8000 Hz was not considered. The first resonant mode (4000 Hz) shows a stable behavior, but it has a

lower amplitude compared to the resonant mode at 6800 Hz. This mode has the highest amplitude, stability, and signal-to-noise ratio (SNR). Consequently, and in order to evaluate the position of the microphones inside the cell, two characterizations were performed. Frequency sweeps were performed in the range previously defined for the microphone position parallel and perpendicular to the input beam, rotating the microphones  $90^\circ$ , as shown in Figure 7a, and evaluating the frequency response. As shown in Figure 7b, the behavior in the measurement range is similar in the two configurations. However, in the configuration perpendicular to the input beam, the amplitude of the main resonant mode is slightly higher (6%).

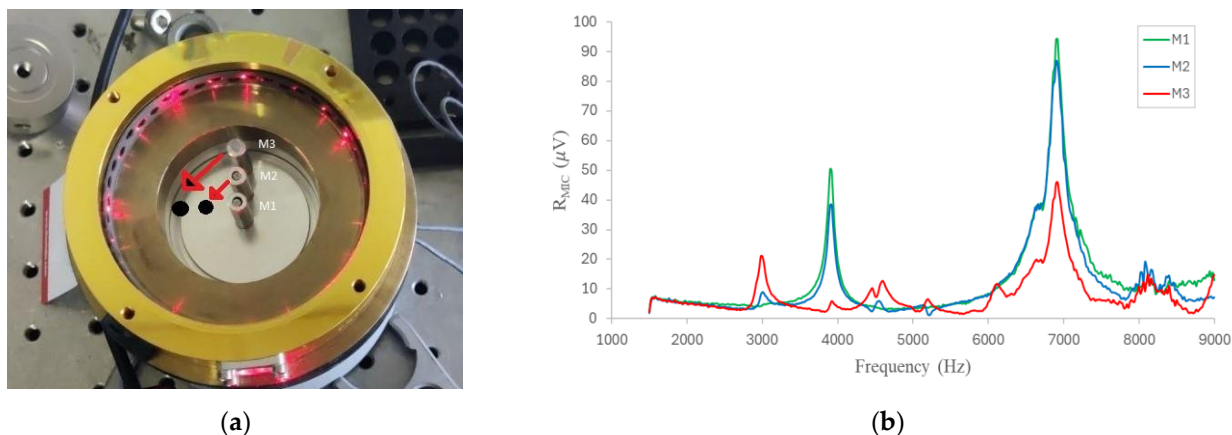


**Figure 7.** (a) Diagram of the installation of the three sensors perpendicular to the optical beam. (b) Resonant modes within the cell identified by the three microphones parallel to the optical beam.

Finally, as shown in Figures 6 and 7, the microphone with the best response is the M1, positioned precisely at the center of the cell, and, thus, it was selected for further measurements. It is imperative to elucidate that the height at which the sensor was installed within the cell was also subjected to evaluation, with the finding that proximity to the center yielded optimal results.

The detailed frequency response of the MPC for the M1 and M2 was determined by performing a frequency sweep from 6 kHz to 7.2 kHz, as illustrated in Figure 8, which is in close proximity to the main resonance frequency that had been determined previously, while varying the chopper modulation frequency in steps of 20 Hz. The resonance frequency ( $f_r$ ) of the MPC was measured to be approximately 6800 Hz, accompanied by a Q factor of approximately 32 at standard atmospheric pressure and room temperature.

### 3.2. Calibration Curve, Sensitivity, and Detection Limits

The excitation laser current was tuned to an  $\text{NH}_3$  absorption line and wavelength modulation (WMS) was implemented by directly modulating the laser using a sinusoidal signal from the lock-in amplifier with a frequency of 3400 Hz, which is half the frequency of the main resonant mode ( $f_r/2$ ). This signal was connected to the laser driver, which allowed for an external modulation connection with a modulation coefficient of 150 mA/V. Subsequently, the acquired signal was demodulated in the second harmonic using the lock-in amplifier, thus performing  $2f$ -WMS detection. The modulation amplitude was varied in a range between 20 mV and 100 mV to find the optimal amplitude that maximizes the central peak value and obtains the best spectral response. Figure 9a shows the detected spectra of the  $2f$ -WMS signal for three different amplitudes, while Figure 9b shows the amplitude value for the central peak (Amplitude 1) and the difference between the main peak and the first peak on the left (Amplitude 2) for 10 different amplitude values. In this way, the optimal modulation amplitude was identified as 60 mV [34].

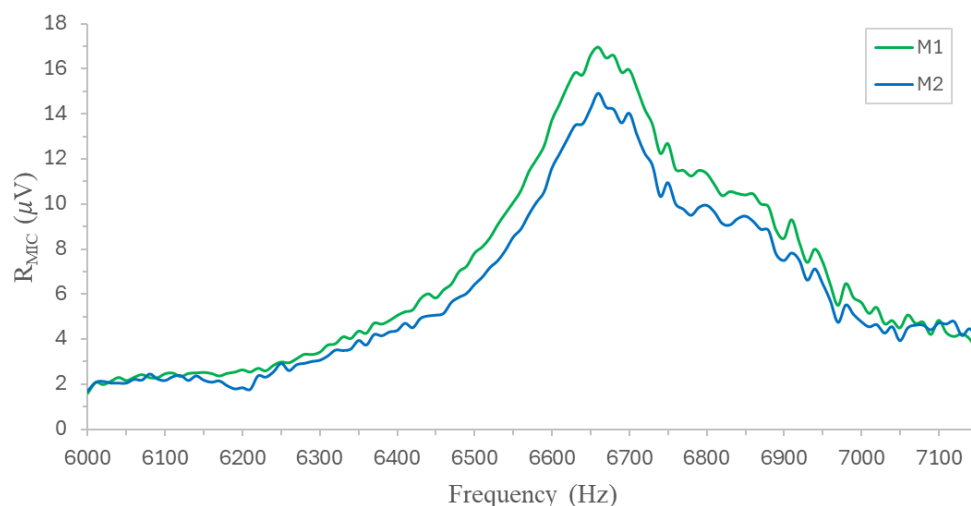


**Figure 8.** Detail of the main resonance mode for sensors M1 and M2.

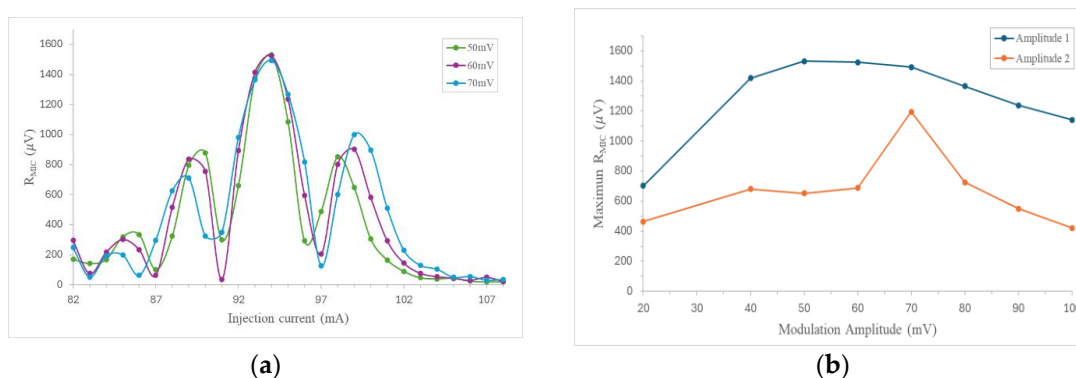


**Figure 9.** (a)  $2f$ -WMS photoacoustic signal for different modulation amplitudes of the same  $\text{NH}_3$  absorption lines. (b)  $2f$ -WMS photoacoustic signal of the main peak amplitude (Amplitude 1) and the difference between the main and secondary peaks on the left (Amplitude 2) as a function of modulation amplitude. All measurements were made with a mixture of 5000 ppmv  $\text{NH}_3$  in  $\text{N}_2$  at atmospheric pressure and room temperature.

As mentioned above, starting from the certified concentration of 5000 ppm  $\text{NH}_3:\text{N}_2$ , different concentrations of  $\text{NH}_3$  were obtained, from 200 ppm to 5000 ppm, using a gas mixer and maintaining a constant flow throughout the measurement of 60 mlm. For each concentration, several spectral sweeps of the  $\text{NH}_3$  absorption line were recorded. Representative  $2f$ -MPC-PAS scans are shown in Figure 10a. The average peak signal values were plotted against  $\text{NH}_3$  concentration. The data set together with the best linear fit, representing the calibration curve of the  $\text{NH}_3$  sensor, is shown in Figure 10b. A coefficient of determination ( $R^2$ ) of 0.987 is obtained, confirming the linearity of the sensor over this range.

Finally, to estimate the noise, a laser wavelength sweep was performed in the measurement range between 84.9 and 103 mA, as shown in Figure 11. The noise level was determined from the signal obtained with the gas cell filled with  $\text{N}_2$  only. This signal was taken every second for 60 s. The data set was then analyzed, and the standard deviation of the noise sample ( $1\sigma$ ) was determined to be  $5.36 \times 10^{-7}$  V. The minimum detection limit (SNR = 1), taking into account the standard deviation of the noise ( $1\sigma$ ), was estimated at 770 ppb, using the ratio between the standard deviation of the background noise and the sensitivity of the system (slope of the calibration curve in Figure 10b). Consequently, the corresponding normalized equivalent absorption coefficient (NNEA) for  $\text{NH}_3$  was  $1.07 \times 10^{-8} \text{ W cm}^{-1} \text{ Hz}^{-1/2}$ , obtained with a bandwidth of 0.26 Hz (for a time constant

of 0.3 s) and an effective power of 30 mW, which was calculated by considering the ratio between the incident power and the output power measured by the reference photodetector.

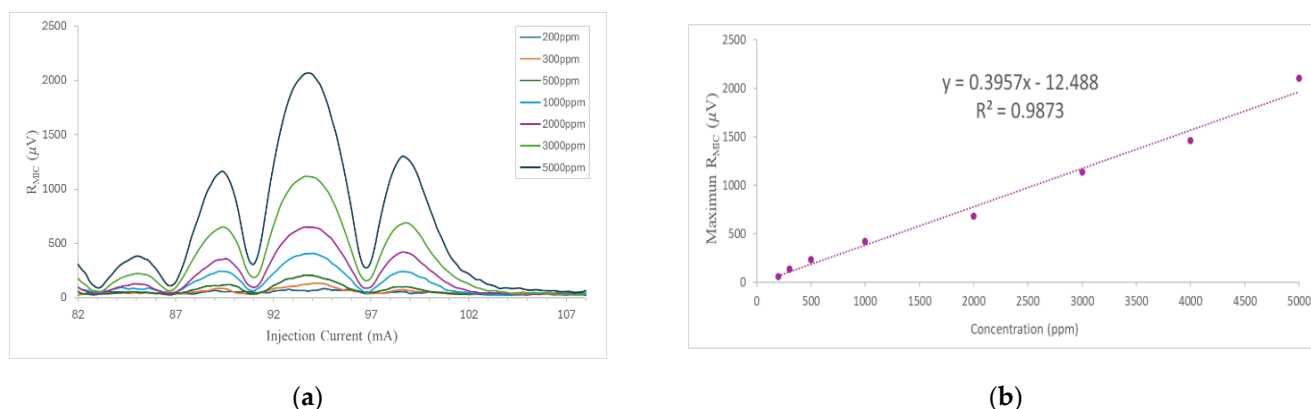


**Figure 10.** Photoacoustic signal measured inside the circular multipass cell for different  $NH_3$  concentrations. (a)  $2f$ -WMS signal for the absorption line under study. (b) Linear fitting. The pressure is set to 1 atm and temperature to 296 K.

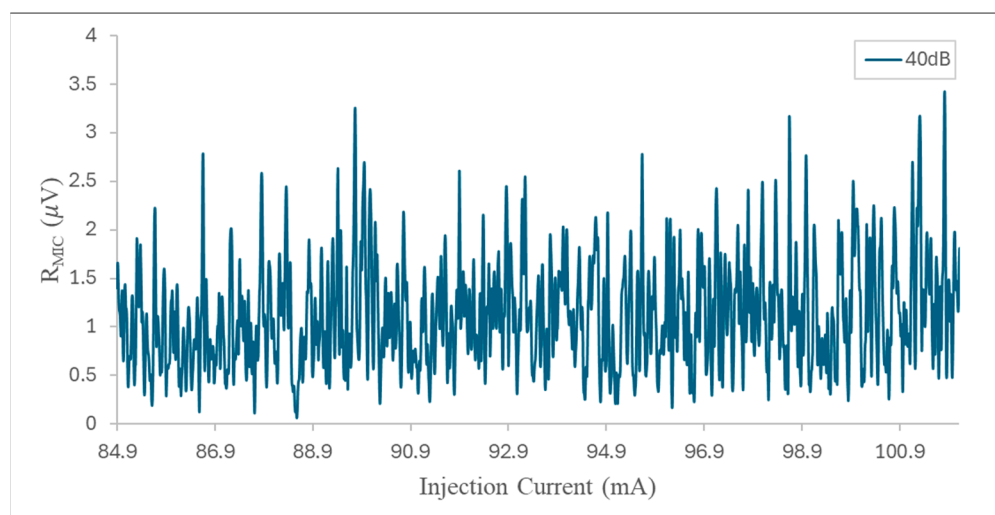


**Figure 11.** Noise signal for the  $2f$ -WMS photoacoustic signal acquired for pure  $N_2$  in a range from 84.9 to 103 mA.

#### 4. Discussion

The system, which uses near-infrared photoacoustic spectroscopy with a 1532 nm semiconductor laser and a multipass cell, has proven to be efficient for gas detection, especially with regard to the detection of ammonia ( $NH_3$ ). The achieved detection limit is approximately 770 ppb, with a normalized noise equivalent absorption coefficient (NNEA) for  $NH_3$  of  $1.07 \times 10^{-8} W cm^{-1} Hz^{-1} / ^2$ . This performance is competitive but also reveals areas for improvement compared to other more advanced approaches.

A comparison with other studies reveals that the multipass cell photoacoustic system demonstrates lower performance in terms of sensitivity and detection limits when compared with the results obtained in studies by Moser [2] and Mürztz et al. [3]. This difference stems from the fact that these systems utilize different technologies and spectral regions, such as quantum cascade lasers (QCL) in the mid-infrared (MIR), and, consequently, achieve lower detection limits and better spectral resolution. For instance, in the study by Moser, a spectroscopy system was employed for the detection of  $H_2S$  with high-precision MIR lasers, resulting in detection limits of less than 1 ppb. However, this

system is limited by the need to use more complex and expensive devices. The use of the multipass cell in this study has the advantage of increasing the optical path, which improves the absorption efficiency and, therefore, the photoacoustic signal. This approach aligns with the research of Liu and Ma [26], who demonstrated that the MPC significantly enhances the sensitivity in the detection of trace gases by facilitating a greater interaction between the gas and the light. However, a critical point is that, although improvements in the signal are achieved, the system remains sensitive to thermal noise and fluctuations in the laser, which can compromise the stability of long-term measurements. This is a crucial consideration, particularly in the context of continuous monitoring applications. Additionally, a significant challenge posed by such systems is the calibration and stability of the laser, a problem that has been highlighted by Graf et al. [27]. Despite the increase in optical path provided by the cell, ensuring wavelength accuracy and signal linearity remains paramount for the accuracy of measurements.

A comparative assessment of techniques such as QEPAS and TDLAS, which use tunable diode lasers, also shows notable differences. In the case of QEPAS, the use of acoustic resonators allows for greater sensitivity and resolution, overcoming the limitations of traditional multipass cells in terms of volume and gas pressure. Tuzson et al. [23] demonstrated that QEPAS can achieve detection limits in the order of ppb for gases such as CO<sub>2</sub> or NO<sub>2</sub>, indicating the potential for further enhancement of photoacoustic based systems with MPCs to achieve comparable detection limits. However, QEPAS systems are more complex, which can limit their practicality for mobile or low-cost applications.

The detection limits in parts per billion (ppb) were obtained through primary calibration in the range of 200 to 5000 ppm. This decision was based on several technical factors that allow valid extrapolation to lower concentrations under controlled conditions. Firstly, the spectroscopic techniques employed delineate a linear relationship between the degree of absorption and the target gas concentration, provided that the signal-to-noise ratio is satisfactory. Furthermore, specific measures have been implemented to mitigate the adsorption/desorption effects characteristic of NH<sub>3</sub> at trace concentrations. These include inert coatings on the cell walls and pipes, and carefully regulated flow rates to ensure homogeneous renewal of the analysis volume. These actions are designed to mitigate non-linear phenomena, memory effects, and long response times that could compromise measurement at the ppb level. Although direct calibration at ultra-low concentrations was not performed at this stage, the detection limit (LOD) was determined experimentally from statistical analysis of background noise and system repeatability under controlled conditions. This approach reliably estimates the sensitivity of the system in the ppb range. However, it is recognized that cross-validation using standard mixtures in the sub-ppm and ppb range will be necessary to empirically confirm the extrapolation of the response. This step is planned as future work and will be presented in subsequent publications.

The results obtained with the MPC-PAS system are very promising, but they also show certain limitations. Despite achievements in improving the optical path and the signal, current technologies still face significant challenges in terms of sensitivity and long-term stability.

However, MPC-PAS systems are more accessible and less complex compared to other approaches, such as systems using quantum cascade lasers (QCL) or QEPAS, making them an excellent option for industrial applications and field measurements. On the other hand, the results show that, in terms of monitoring industrial gases or ammonia emissions, the multipass cell photoacoustic system could be an efficient and cost-effective option. The enhancement of signal by increasing the optical path is a strategy that has proven effective and is worthy of further optimization. As previously mentioned, the mid-infrared offers deeper absorption lines for a wider range of gases, which would improve sensitivity and

lower detection limits. Recent research, such as that of Patimisco et al. [23], suggests that the transition to MIR could be the key to overcoming the limitations of near-infrared photoacoustic systems. This transition would not only enhance the detection of gases such as  $\text{NH}_3$ , but also address gases of industrial interest, including  $\text{H}_2\text{S}$  and  $\text{NO}_2$ , which exhibit more pronounced absorption characteristics in the MIR. The miniaturization of photoacoustic spectroscopy systems has the potential to unlock new applications, particularly in real-time environmental monitoring. According to Manninen et al. [28], compact MPCs and portable systems are beginning to have a significant impact on gas monitoring in the field. The development of portable systems that can perform real-time measurements without sacrificing accuracy would represent a key advance.

## 5. Conclusions

The results obtained with the photoacoustic system, based on a 1532 nm semiconductor laser and a multipass cell, demonstrated an effective capacity for gas detection, particularly ammonia ( $\text{NH}_3$ ). The minimum detection limit of 770 ppb was achieved, with a standard deviation of noise of  $5.36 \times 10^{-7}$  V and a noise-normalized equivalent absorption coefficient (NNEA) of  $1.07 \times 10^{-8} \text{ W cm}^{-1} \text{ Hz}^{-1/2}$ . These values were determined under controlled conditions, using a cell with pure  $\text{N}_2$  and statistical analysis of the noise recorded over 60 s. While this performance is competitive with certain optical detection methods, it falls short of more advanced techniques, such as those using mid-infrared (MIR) quantum cascade lasers, which can achieve sub-ppb detection limits.

MPC-PAS offers several significant advantages over other gas detection devices. Firstly, the circular multipass geometry allows the effective optical path to be substantially increased without increasing the volume of the cell, which improves the sensitivity of the system by amplifying the amount of energy absorbed by the gas. This, when combined with photoacoustic detection, which directly converts optical absorption into a proportional acoustic signal, allows very low detection limits (even in the ppb range) to be achieved with high spectral specificity, in contrast to NIR or fiber optic sensors, which generally have lower spectral resolution and are more prone to background interference. In addition, in comparison with conventional sensors that rely on chemical reactions or electrical properties, photoacoustic spectroscopy is not dependent on the degradation of reactive materials. This results in enhanced long-term stability and a reduced requirement for frequent recalibration [28,35].

Notwithstanding, the proposed system exhibits distinct advantages in terms of simplicity, cost, and adaptability for industrial and field monitoring applications. Whilst QCL- or QEPAS-based technologies offer superior sensitivity, they also involve a greater degree of complexity and cost, which limits their use in practical environments. The enhancement of the system through the implementation of a multipass cell has been demonstrated to be a successful strategy for achieving sensitivity enhancement without the necessity for highly sophisticated devices. Furthermore, the results suggest that a future transition to the mid-infrared region, combined with miniaturization and laser stabilization techniques, could significantly increase the performance of portable photoacoustic systems. This, in turn, could enable new applications in real-time environmental monitoring and industrial emissions control.

**Author Contributions:** Conceptualization, O.E.B.-M. and J.V.P.; methodology, O.E.B.-M.; software, A.P.G.-B. and J.V.P.; validation, O.E.B.-M. and J.V.P.; data curation, J.V.P., A.P.G.-B., and G.D.; writing—original draft preparation, O.E.B.-M.; writing—review and editing, O.E.B.-M., J.V.P., and G.D.; visualization, A.P.G.-B.; supervision, O.E.B.-M.; funding acquisition, O.E.B.-M. and G.D. All authors have read and agreed to the published version of the manuscript.

**Funding:** The first and fourth authors are supported by the Grants for research activity of young PhD holders, part of the Universidad Carlos III de Madrid (UC3M) Own Research Program (Ayudas para la Actividad Investigadora de los Jóvenes Doctores, del Programa Propio de Investigación de la UC3M - Proyectos Jóvenes PPIT2024). Furthermore, they disclosed receipt of the following financial support for the research, authorship, and/or publication of this article: This work has been supported by the Madrid Government (Comunidad de Madrid—Spain) under the Multiannual Agreement with the UC3M (IA\_aCTRI-CM-UC3M).

**Institutional Review Board Statement:** Not applicable.

**Informed Consent Statement:** Not applicable.

**Data Availability Statement:** Dataset available on request from the authors. The raw data supporting the conclusions of this article will be made available by the authors on request.

**Acknowledgments:** To student Sergio Paniagua for his initial research on the subject, and to manager Wilman Chávez for his help with layout and editing. Finally, to Pedro Martín-Mateos, for his support and assistance in all aspects.

**Conflicts of Interest:** The authors declare no conflicts of interest.

## Abbreviations

The following abbreviations are used in this manuscript:

PAS	Photoacoustic Spectroscopy
NH <sub>3</sub>	Ammonia
N <sub>2</sub>	Nitrogen
CO <sub>2</sub>	Carbon Dioxide
NO <sub>2</sub>	Nitrogen Dioxide
H <sub>2</sub> S	Hydrogen Sulfide
GHG	Greenhouse Gas
NNEA	Normalized Noise Equivalent Absorption
QCL	Quantum Cascade Laser
QEPAS	Quartz-Enhanced Photoacoustic Spectroscopy
CEPAS	Cantilever-Enhanced Photoacoustic Spectroscopy
VOCs	Volatile Organic Compounds
TDLAS	Tunable Diode Laser Absorption Spectroscopy
DFB-CW	Distributed Feedback Continuous Wave
MPC	Multipass Cell
NIR	Near-Infrared
MIR	Mid-Infrared
SNR	Signal-to-Noise Ratio
WMS	Wavelength Modulation Spectroscopy

## References

1. Milone, A.; Monteduro, A.G.; Rizzato, S.; Leo, A.; Maruccio, G. Gas Sensing Technologies—Status, Trends, Perspectives and Novel Applications. *arXiv* **2021**, arXiv:2110.13637. [[CrossRef](#)]
2. Moser, H. Development and Implementation of an Industrial Process Gas Monitoring System for H<sub>2</sub>S Based on Mid-Infrared Quantum Cascade Laser Spectroscopy. Ph.D. Dissertation, Technische Universität Wien, Vienna, Austria, 2016. [[CrossRef](#)]
3. Mürtz, M.; Halmer, D.; Horstjann, M.; Thelen, S.; Hering, P. Ultra Sensitive Trace Gas Detection for Biomedical Applications. *Spectrochim. Acta Part A Mol. Biomol. Spectrosc.* **2006**, *63*, 963–969. [[CrossRef](#)] [[PubMed](#)]
4. Amann, A.; de Lacy Costello, B.; Miekisch, W.; Schubert, J.; Buszewski, B.; Pleil, J.; Ratcliffe, N.; Risby, T. The Human Volatilome: Volatile Organic Compounds (VOCs) in Exhaled Breath, Skin Emanations, Urine, Feces and Saliva. *J. Breath. Res.* **2014**, *8*, 034001. [[CrossRef](#)] [[PubMed](#)]
5. Chang, J.E.; Lee, D.S.; Ban, S.W.; Oh, J.; Jung, M.Y.; Kim, S.H.; Park, S.J.; Persaud, K.; Jheon, S. Analysis of Volatile Organic Compounds in Exhaled Breath for Lung Cancer Diagnosis Using a Sensor System. *Sens. Actuators B Chem.* **2018**, *255*, 800–807. [[CrossRef](#)]

6. Crow, D.J.G.; Balcombe, P.; Brandon, N.; Hawkes, A.D. Assessing the Impact of Future Greenhouse Gas Emissions from Natural Gas Production. *Sci. Total Environ.* **2019**, *668*, 1242–1258. [CrossRef]
7. Yin, L.; Tao, F.; Zhai, R.; Chen, Y.; Hu, J.; Wang, Z.; Fu, B. Impacts of Future Climate Change and Atmospheric CO<sub>2</sub> Concentration on Ecosystem Water Retention Service. *Earth's Future* **2022**, *10*, e2021EF002138. [CrossRef]
8. Rocha, R.C.; Costa, M.; Bai, X.S. Combustion and Emission Characteristics of Ammonia under Conditions Relevant to Modern Gas Turbines. *Combust. Sci. Technol.* **2021**, *193*, 2514–2533. [CrossRef]
9. Li, J.; Lai, S.; Chen, D.; Wu, R.; Kobayashi, N.; Deng, L.; Huang, H. A Review on Combustion Characteristics of Ammonia as a Carbon-Free Fuel. *Front. Energy Res.* **2021**, *9*, 760356. [CrossRef]
10. UK Health Security Agency. *Ammonia: Toxicological Overview*; UK Health Security Agency: London, UK, 2024. Available online: <https://www.gov.uk/government/publications/ammonia-properties-incident-management-and-toxicology/ammonia-toxicological-overview> (accessed on 14 May 2025).
11. Yapicioglu, A.; Dincer, I. A Review on Clean Ammonia as a Potential Fuel for Power Generators. *Renew. Sustain. Energy Rev.* **2019**, *103*, 96–108. [CrossRef]
12. Salmon, N.; Bañares-Alcántara, R. Green Ammonia as a Spatial Energy Vector: A Review. *Sustain. Energy Fuels R. Soc. Chem.* **2021**, *5*, 2814–2839. [CrossRef]
13. Gupta, P.; Maurya, S.; Pandey, N.K.; Verma, V. Metal-Oxide Based Ammonia Gas Sensors: A Review. *Nanosci. Nanotechnol. -Asia* **2021**, *11*, 270–289. [CrossRef]
14. Zhimin, P.; Yanjun, D.; Lu, C.; Xiaohang, L.; Kangjie, Z. Calibration-Free Wavelength Modulated TDLAS under High Absorbance Conditions. *Opt. Express* **2011**, *19*, 23104–23110. [CrossRef] [PubMed]
15. Sun, K.; Chao, X.; Sur, R.; Goldenstein, C.S.; Jeffries, J.B.; Hanson, R.K. Analysis of Calibration-Free Wavelength-Scanned Wavelength Modulation Spectroscopy for Practical Gas Sensing Using Tunable Diode Lasers. *Meas. Sci. Technol.* **2013**, *24*, 125203. [CrossRef]
16. Thakur, S.N. Photoacoustic and Photothermal Spectroscopy. In *Photoacoustic and Photothermal Spectroscopy: Principles and Applications*; Elsevier: Amsterdam, The Netherlands, 2022; pp. 1–19. [CrossRef]
17. Rai, V.N.; Thakur, S.N. Physics and Instrumentation of Photothermal and Photoacoustic Spectroscopy of Solids. In *Photoacoustic and Photothermal Spectroscopy: Principles and Applications*; Elsevier: Amsterdam, The Netherlands, 2022; pp. 21–49. [CrossRef]
18. Elia, A.; Lugarà, P.M.; di Franco, C.; Spagnolo, V. Photoacoustic Techniques for Trace Gas Sensing Based on Semiconductor Laser Sources. *Sensors* **2009**, *9*, 9616–9628. [CrossRef]
19. Bonilla-Manrique, O.E.; Posada-Roman, J.E.; Garcia-Souto, J.A.; Ruiz-Llata, M. Sub-Ppm-Level Ammonia Detection Using Photoacoustic Spectroscopy with an Optical Microphone Based on a Phase Interferometer. *Sensors* **2019**, *19*, 2890. [CrossRef]
20. Bonilla-Manrique, O.E.; Moser, H.; Martín-Mateos, P.; Lendl, B.; Ruiz-Llata, M. Hydrogen Sulfide Detection in the Midinfrared Using a 3d-Printed Resonant Gas Cell. *J. Sens.* **2019**, *2019*, 6437431. [CrossRef]
21. Varga, A.; Bozóki, Z.; Szakáll, M.; Szabó, G. Photoacoustic System for On-Line Process Monitoring of Hydrogen Sulfide (H<sub>2</sub>S) Concentration in Natural Gas Streams. *Appl. Phys. B* **2006**, *85*, 315–321. [CrossRef]
22. He, Y.; Ma, Y.; Tong, Y.; Yu, X.; Tittel, F.K. HCN Ppt-Level Detection Based on a QEPAS Sensor with Amplified Laser and a Miniaturized 3D-Printed Photoacoustic Detection Channel. *Opt. Express* **2018**, *26*, 9666–9675. [CrossRef]
23. Patimisco, P.; Scamarcio, G.; Tittel, F.K.; Spagnolo, V. Quartz-Enhanced Photoacoustic Spectroscopy: A Review. *Sensors* **2014**, *14*, 6165–6206. [CrossRef]
24. Qiao, S.; He, Y.; Sun, H.; Patimisco, P.; Sampaolo, A.; Spagnolo, V.; Ma, Y. Ultra-Highly Sensitive Dual Gases Detection Based on Photoacoustic Spectroscopy by Exploiting a Long-Wave, High-Power, Wide-Tunable, Single-Longitudinal-Mode Solid-State Laser. *Light Sci. Appl.* **2024**, *13*, 100. [CrossRef]
25. Gagliardi, G.; Loock, H.-P. *Cavity-Enhanced Spectroscopy and Sensing*; Springer: Berlin/Heidelberg, Germany, 2014. [CrossRef]
26. Moser, H.; Lendl, B. Cantilever-Enhanced Photoacoustic Detection of Hydrogen Sulfide (H<sub>2</sub>S) Using NIR Telecom Laser Sources near 1.6 Mm. *Appl. Phys. B Lasers Opt.* **2016**, *122*, 83. [CrossRef]
27. Liu, Y.; Ma, Y. Advances in Multipass Cell for Absorption Spectroscopy-Based Trace Gas Sensing Technology [Invited]. *Chin. Opt. Lett.* **2023**, *21*, 33001. [CrossRef]
28. Wang, L.; Zhang, T.; Huang, Y.; Zheng, Y.; Wang, G.; He, S. Enhanced Photoacoustic Spectroscopy Integrated with a Multi-Pass Cell for Ppb Level Measurement of Methane. *Appl. Sci.* **2024**, *14*, 6068. [CrossRef]
29. Graf, M.; Emmenegger, L.; Tuzson, B. Compact, Circular, and Optically Stable Multipass Cell for Mobile Laser Absorption Spectroscopy. *Opt. Lett.* **2018**, *43*, 2434. [CrossRef]
30. Manninen, A.; Tuzson, B.; Looser, H.; Bonetti, Y.; Emmenegger, L. Versatile Multipass Cell for Laser Spectroscopic Trace Gas Analysis. *Appl. Phys. B Lasers Opt.* **2012**, *109*, 461–466. [CrossRef]
31. Tuzson, B.; Mangold, M.; Looser, H.; Manninen, A.; Emmenegger, L. Compact Multipass Optical Cell for Laser Spectroscopy. *Opt. Lett.* **2013**, *38*, 257–266. [CrossRef]

32. Rothbart, N.; Schmalz, K.; Hubers, H.W. A Compact Circular Multipass Cell for Millimeter-Wave/Terahertz Gas Spectroscopy. *IEEE Trans. Terahertz Sci. Technol.* **2020**, *10*, 9–14. [[CrossRef](#)]
33. Mangold, M.; Tuzson, B.; Hundt, M.; Jágerská, J.; Looser, H.; Emmenegger, L. Circular Paraboloid Reflection Cell for Laser Spectroscopic Trace Gas Analysis. *J. Opt. Soc. Am. A* **2016**, *33*, 913. [[CrossRef](#)]
34. de Matos, M.A.A.; da Silva Ferreira, V. Gas Mass-Flow Meters: Principles and Applications. *Flow Meas. Instrum.* **2010**, *21*, 143–149. [[CrossRef](#)]
35. Wijesinghe, D.R.; Zobair, M.A.; Esmaeelpour, M. A Review on Photoacoustic Spectroscopy Techniques for Gas Sensing. *Sensors* **2024**, *24*, 6577. [[CrossRef](#)]

**Disclaimer/Publisher's Note:** The statements, opinions and data contained in all publications are solely those of the individual author(s) and contributor(s) and not of MDPI and/or the editor(s). MDPI and/or the editor(s) disclaim responsibility for any injury to people or property resulting from any ideas, methods, instructions or products referred to in the content.